Environmental Science Processes & Impacts

ROYAL SOCIETY OF CHEMISTRY

PAPER

View Article Online
View Journal | View Issue

Cite this: *Environ. Sci.: Processes Impacts*, 2024, **26**, 519

Atmospheric mercury uptake and accumulation in forests dependent on climatic factors†

Yo Han Yang, [a] Min-Seob Kim, [b] Jaeseon Park [b] and Sae Yun Kwon *[a]

The environmental and climatic factors dictating atmospheric mercury (Hg) uptake by foliage and accumulation within the forest floor are evaluated across six mountain sites, South Korea, using Hg concentration and Hg stable isotope analyses. The isotope ratios of total gaseous Hg (TGM) at six mountains are explained by local anthropogenic Hg emission influence and partly by mountain elevation and wind speed. The extent to which TGM is taken up by foliage is not dependent on the site-specific TGM concentration, but by the local wind speed, which facilitates TGM passage through dense deciduous canopies in the Korean forests. This is depicted by the significant positive relationship between wind speed and foliage Hg concentration ($r^2 = 0.92$, $p < 0.05$) and the magnitude of δ^{202}Hg shift from TGM to foliage ($r^2 = 0.37$, $p > 0.05$), associated with TGM uptake and oxidation by foliar tissues. The litter and topsoil Hg concentrations and isotope ratios reveal relationships with a wide range of factors, revealing lower Hg level and greater isotopic fractionation at sites with low elevation, high wind speed, and high mean warmest temperature. We attribute this phenomenon to active TGM re-emission from the forest floor at sites with high wind speed and high temperature, caused by turnover of labile organic matter and decomposition. In contrast to prior studies, we observe no significant effect of precipitation on forest Hg accumulation but precipitation appears to reduce foliage-level Hg uptake by scavenging atmospheric Hg species available for stomata uptake. The results of this study would enable better prediction of future atmospheric and forest Hg influence under climate change.

Received 17th October 2023
Accepted 29th January 2024

DOI: 10.1039/d3em00454f

rsc.li/espi

Environmental significance

Forests are recognized as a global sink for mercury, by removing atmospheric mercury *via* the stomata uptake by foliage. Our study aims to identify key environmental and climatic factors affecting foliar Hg uptake and accumulation within the forest floor across six mountain sites, South Korea. The measurement of mercury concentration and mercury stable isotopes suggests that local wind speed is the dominant predictor of foliage mercury level and the associated isotopic fractionation, rather than site-specific atmospheric mercury concentration. Forest floor mercury concentration and isotope ratios are influenced by climatic factors (wind speed, air temperature), which enhance decomposition and subsequent Hg re-emission from litter and soil. The identified factors can be used to predict future impacts of atmospheric mercury in forest ecosystems.

1. Introduction

Biogeochemical cycling and fate of atmospheric mercury (Hg) in forests have been studied extensively in the recent decade.[1,2] This is because forests act as a major sink for atmospheric Hg, by taking up 1500 to 2100 Mg Hg year^{-1} from the atmosphere.[3] The primary pathway in which atmospheric Hg is taken up by forests is through the sequestration of gaseous elemental Hg^0 *via* stomata in foliage.[4,5] Non-stomatal Hg^0 uptake *via* foliage cuticles has also been reported at night[6] and in coniferous canopies.[7] Hg^0 has a long residence time and is well-mixed in the atmosphere, making it broadly available for uptake by forests and other aquatic and terrestrial surfaces.[8] Direct Hg^0 uptake by the forest floor has recently been identified as an overlooked pathway, accounting for over half of the total atmospheric Hg^0 uptake in mid-latitude forests.[9] Conversely, wet and dry Hg deposition, in the form of oxidized Hg^{2+} and particulate bound Hg (PBM), onto foliage, litter, and soil surfaces constitutes relatively small proportions.[4,10]

Recent applications of stable Hg isotopes have shed light on specific biogeochemical processes governing atmospheric Hg transformation, accumulation, and re-emission in forests. Mass-dependent fractionation (MDF) or changes in δ^{202}Hg, which is known to occur *via* all-known Hg biogeochemical processes, have been documented during Hg^0 uptake and oxidation *via* foliar tissues,[10] Hg^0 re-emission,[11,12] and dark

[a]*Division of Environmental Science and Engineering, Pohang University of Science and Technology, 77 Cheongam-Ro, Nam-Gu, Pohang 37673, South Korea. E-mail: saeyunk@postech.ac.kr; Fax: +82-54-279-8299; Tel: +82-54-279-2290*

[b]*Environmental Measurement & Analysis Center, National Institute of Environmental Research, 42 Hwangyong-Ro, Seo-Gu, Incheon 22689, South Korea*

† Electronic supplementary information (ESI) available. See DOI: https://doi.org/10.1039/d3em00454f

abiotic and microbial reductions within soil.[13–15] Mass-independent fractionation (MIF) or changes in Δ^{199}Hg and Δ^{200}Hg occur primarily *via* Hg^{2+} photo-reduction[16] and Hg^0 photo-oxidation,[17] respectively, and have been used to identify processes leading to Hg^0 re-emission from foliage and forest floor[11,15] and for distinguishing between atmospheric Hg species (Hg^0 *vs.* Hg^{2+}) affecting forest media.[18] Dark abiotic redox processes are also known to cause small changes in Δ^{199}Hg.[19,20]

The extent to which the aforementioned biogeochemical processes occur depends on environmental and climatic factors, which subsequently dictate the fate of atmospheric Hg^0 within forests. Across a large spatial scale (national to regional level), precipitation and soil carbon content are regarded to be the strongest predictors of spatial variability in atmospheric Hg^0 accumulation in the forest floor.[1,2,21–24] Regions of frequent and high levels of precipitation are thought to have active biomass production, which, in turn, increase foliage available for Hg^0 uptake and delivery to soil *via* litterfall. Using a passive exchange meter device, Zhang *et al.*[25] also reported that temperature and humidity can facilitate Hg^0 re-emission from forest litter by mediating rapid turnover of labile organic matter. Relative to the forest floor, the environmental/climatic factors affecting Hg^0–foliage interaction over a large spatial scale is less well constrained, although the diurnal and temporal profiles of Hg^0 fluxes over canopy are well documented.[7,9,15,26] Among a handful of studies, B. Wang *et al.*[12] reported positive correlations between foliage Hg^0 uptake and temperature and solar radiation, and negative correlations with humidity and air Hg^0 concentration over the canopy in a remote mountain, China. We speculate that foliar Hg^0 uptake is more sensitive to changes in environmental/climatic factors and may serve as an additional predictor of spatial Hg^0 accumulation across forests.

Our study evaluates environmental/climatic factors affecting atmospheric Hg^0 level and its uptake and accumulation across six South Korean forests. Identifying key factors is critical in South Korea given that >60% of land is occupied by forested mountains.[27] Despite the substantial domestic anthropogenic Hg emissions and proximity to Hg emitting countries in East Asia, low atmospheric Hg^0 concentrations reported across the nation[28] are suspected to be driven by active foliage Hg^0 uptake. Here, we sampled total gaseous Hg (TGM; Hg^0 + Hg^{2+}), foliage, litter, and topsoil at the highest elevation of six mountain sites in South Korea. The same genus of vegetative species (*Quercus*) was sampled for foliage and litter and in the same month of the year (July) to minimize the effect of tree physiological processes and seasonal variations on Hg accumulation. The TGM concentration and isotope ratios are evaluated in relation to climatic/environmental factors and compared with foliage to identify key indicators governing foliar Hg^0 uptake. The Hg isotope ratios of foliage, litter, and topsoil are also compared within and across the mountain sites to assess Hg^0 fate and factors dictating soil Hg input. The results of this study would enable interpretation of atmospheric Hg^0 concentrations over South Korea and for predicting future atmospheric and forest Hg^0 influences under climate change.

2. Methods

2.1. Site description

It is estimated that >60% of the land cover in South Korea is dominated by deciduous mountains, making South Korea an effective sink for atmospheric Hg^0. We selected six mountains distributed across South Korea, which are characterized as temperate broadleaf and mixed forests of coniferous forests (37%), deciduous forests (32%), and mixed forests (26%).[27] The sampling locations of six mountains are illustrated in Fig. 1 and Table S1,† which were obtained from the Korea Meteorological Administration Weather Data Service website (**https://data.kma.go.kr**), located 7 to 30 km away from the sampling locations. The relative humidity and wind speed are the average values of the sampling month (July) for their respective years of sampling. In addition to their widespread geographical distribution, the mountains selected for this study vary in their proximity to anthropogenic Hg emission sources. Mt Mani, Mt Seokmun, and Mt Gaya are located on the west coast and receive southwesterly wind in summer. Three mountains are in proximity to coal-fired power plants.[29] Mt Bihak and Mt Hambaek are located on the east coast and are situated <20 km away from steel manufacturing plants and cement clinker production facilities. Mt Jiri is located inland and is a relatively remote site, given that anthropogenic Hg emission sources are situated >50 km away from this region.

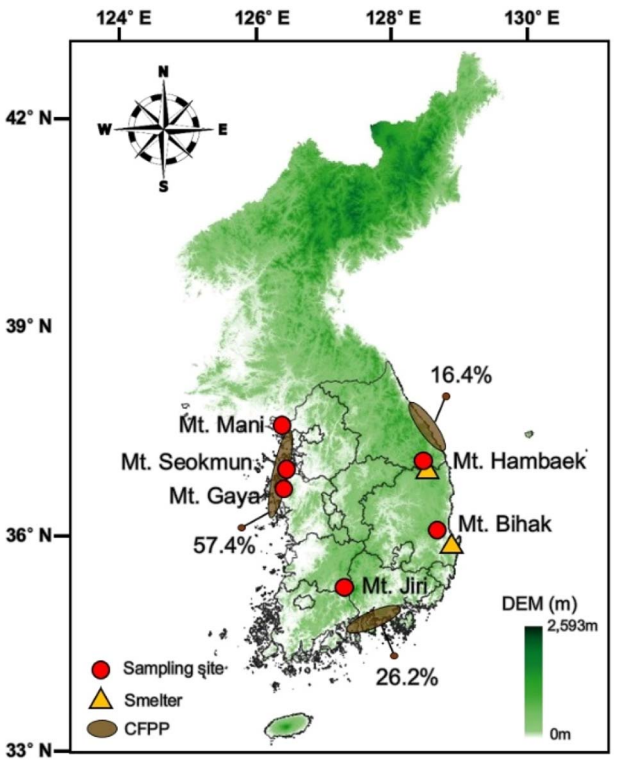

Fig. 1 Locations of six mountain sites in South Korea. CFPP refers to coal-fired power plant and numbers denote % number of coal-fired power plants in a given location from the total national number of CFPP (n = 61). DEM (Digital Elevation Model) represents the height above the sea level.

2.2. Sample collection

In July of 2019 to 2022, TGM, foliage, litter, and topsoil were sampled at the highest elevations (460–1340 m from the sea level) of each mountain site (Table S1†). TGM was collected for three consecutive days for 8 hours (between 8:00 and 16:00 LST) and at 2 m above from the forest floor. TGM was sampled by pumping ambient air *via* an air pump (Flite 3, SKC Inc., USA) onto a gold coated bead trap and at a flow rate of 1.4 L min^{-1} through a PTFE syringe filter inlet (CHMLab., Spain). Prior to TGM collection, each gold trap was heated to 600 °C for 20 min to remove residual Hg. *Quercus dentata* (*Daimyo oak*), *Quercus mongolica* (*Mongolian oak*), and *Quercus aliena* (*galcham oak*) (average height of 4 m) were selected as the target species for foliage and litter given their abundance in South Korea (>30% of the tree biomass in South Korea; 2 002 150 ha)[27] and to minimize the effect of tree physiological processes governing foliar Hg uptake. At each mountain site, a total of 20 L of foliage and litter were sampled, respectively, from multiple trees. Fresh foliage was sampled from a tree branch 2 m above the forest floor (mid canopy) and decomposing litter was collected from the forest floor. Decomposing litter was chosen to evaluate the effect of environmental/climatic factors on the changes in litter Hg concentration and their isotopic compositions. After removing the litter, we used a stainless-steel spade to sample topsoil (0–10 cm). All samples were sealed in polyethylene bags and transported to the Environmental & Health Assessment Laboratory, POSTECH, where they were rinsed with DI, air-dried, stored at −20°C, freeze-dried, and homogenized.

2.3. Hg concentration and isotope analyses

For solid samples (foliage, litter, topsoil), total Hg (THg) concentration was analyzed by atomic absorption spectroscopy (AAS) using a Nippon Instruments MA-3000. The standard reference material (ERM CE 464; tuna fish, TORT-3; lobster, NIST 2711a; Montana II soil) and sample duplicates were included for quality control and quality assurance. The recoveries ranged between 90 and 106% for ERM CE 464 ($n = 14$), 93–109% for TORT-3 ($n = 30$), and 99–110% for NIST 2711a ($n = 11$). The relative standard deviations of sample duplicates ($n = 28$) were within 5%. TGM collected onto a gold trap was desorbed at 600 °C for 10 min and preconcentrated into a 1% $KMnO_4$ (in 10% trace metal grade H_2SO_4) solution and measured for THg by cold vapor atomic fluorescence spectrometry (CV-AFS) (Brooks Rand) according to the US EPA method 1631.[30] The calibration standard ($HgCl_2$, Brooks Rand) was measured between samples, which yielded recoveries between 87 and 110% ($n = 27$).

For Hg isotopes, 0.2–1.4 g of freeze-dried and homogenized foliage, litter, and topsoil were loaded onto a ceramic boat and into a double-stage thermal combustion furnace to release Hg^0. The released Hg^0 was preconcentrated into a 1% $KMnO_4$ solution, following the procedure by Blum and Johnson.[31] Hg in the trapping solution was analyzed using a CV-AFS, which yielded recoveries of 95 ± 13% ($n = 43$) relative to THg measured *via* AAS. Hg isotopes were measured using a multi-collector inductively coupled plasma mass spectrometer (MC-ICP-MS, Nu Instruments, UK). The trapping solution was neutralized with NH_2–OH–HCl and diluted to 1–3 ng Hg mL^{-1} using the same matrix as the trapping solution. The sample was introduced by continuously reducing Hg with 2% $SnCl_2$ and by separating Hg^0 using a glass gas–liquid phase separator. Instrumental mass bias was corrected using an internal Tl standard (NIST 997) and by bracketing samples with NIST 3133 matched to the sample matrix. MDF is reported as δ^{202}Hg values in permil (‰) relative to the NIST 3133:

$$\delta^{202}\mathrm{Hg} = \{[(^{202}\mathrm{Hg}/^{198}\mathrm{Hg})_{\mathrm{sample}}/(^{202}\mathrm{Hg}/^{198}\mathrm{Hg})_{\mathrm{NIST3133}}] - 1\} \times 1000 \quad (1)$$

MIF is reported using a capital delta notation and was calculated using the following equations.[32]

$$\Delta^{199}\mathrm{Hg}\ (‰) = \delta^{199}\mathrm{Hg} - (\delta^{202}\mathrm{Hg} \times 0.2520) \quad (2)$$

$$\Delta^{200}\mathrm{Hg}\ (‰) = \delta^{200}\mathrm{Hg} - (\delta^{202}\mathrm{Hg} \times 0.5024) \quad (3)$$

$$\Delta^{201}\mathrm{Hg}\ (‰) = \delta^{201}\mathrm{Hg} - (\delta^{202}\mathrm{Hg} \times 0.7520) \quad (4)$$

Analytical uncertainty at 2 standard deviation (2SD) is estimated based on replicate analyses of either NIST RM 8610 ($n = 40$), ERM CE 464 ($n = 1$), TORT-3 ($n = 4$), or NIST 2711a ($n = 5$). We chose NIST 2711a because it had the largest uncertainty. Hg isotope ratios of NIST RM 8610 were −0.53 ± 0.04‰ for δ^{202}Hg, −0.02 ± 0.01‰ for Δ^{199}Hg, −0.03 ± 0.02‰ for Δ^{201}Hg, and 0.01 ± 0.01‰ for Δ^{200}Hg. TORT-3 had δ^{202}Hg of 0.04 ± 0.02‰, Δ^{199}Hg of 0.62 ± 0.03‰, Δ^{201}Hg of 0.49 ± 0.06, and Δ^{200}Hg of 0.05 ± 0.01‰. NIST 2711a had δ^{202}Hg of −0.08 ± 0.05‰, Δ^{199}Hg of −0.23 ± 0.01‰, Δ^{201}Hg of −0.18 ± 0.02, and Δ^{200}Hg of −0.02 ± 0.01‰. Hg isotope ratios of all standards are summarized in Table S2† and compared with the values from other laboratories. Pearson's correlation coefficient test (two-tailed) and linear regression were applied to analyze the relationship between THg, climatic factors, and magnitude of isotopic shift using Microsoft Excel 2019. Correlation coefficients and statistical tests with values above 0.05 are considered significant, while those below 0.05 are considered insignificant, unless otherwise specified.

3. Results & discussion

3.1. Total gaseous mercury (TGM)

The TGM collected in this study range between 0.39 and 6.01 ng m^{-3} ($n = 28$). Across the mountain sites, there are no distinct geographical differences (west *vs.* east) in TGM concentrations or by proximity to local anthropogenic Hg emission sources (Table S3†). Instead, the TGM concentration displays a weak but positive relationship with the site-specific elevation ($r^2 = 0.19$, $p > 0.05$) and a negative relationship with the wind speed ($r^2 = 0.11$, $p > 0.05$).

In regard to Hg isotopes, our TGM displays δ^{202}Hg (−1.51 to 0.10‰), Δ^{199}Hg (−0.70 to 0.17‰), and Δ^{200}Hg values (−0.10 to 0.02‰) that are within the ranges of TGM isotope ratios compiled previously over various urban-industrial and remote locations around the world[33] (Fig. 2A and B). The urban-

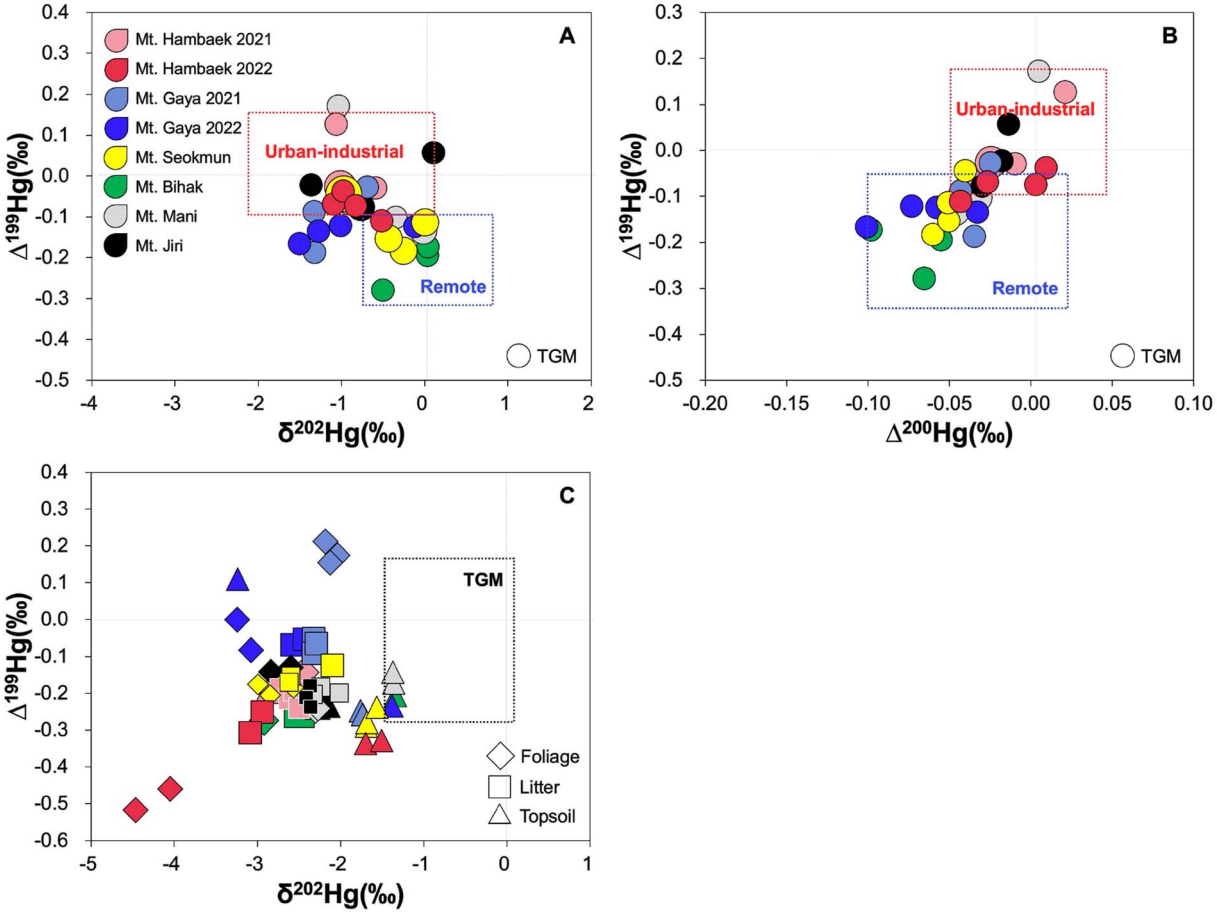

Fig. 2 (A) δ^{202}Hg and Δ^{199}Hg, (B) Δ^{200}Hg and Δ^{199}Hg of all TGM and (C) δ^{202}Hg and Δ^{199}Hg of all foliage, litter, and topsoil sampled across six mountain sites in South Korea.

industrial and remote locations were designated based on the site description of individual compiled studies by Kwon *et al.*[33] The δ^{202}Hg and Δ^{199}Hg of our TGM exhibit intermediate values to that of urban-industrial and remote sites, reflecting mixtures of anthropogenically emitted and long-range or background TGM sources. The Δ^{199}Hg and Δ^{200}Hg, used to distinguish the relative proportion of Hg^0 and Hg^{2+},[17] indicate that our TGM is mostly in the form of Hg^0. Furthermore, the correlation between the TGM concentration (in 1/THg) and Hg isotope ratios reveal increasing TGM concentration with increasing Δ^{199}Hg ($r^2 = 0.58$, $p < 0.05$) and Δ^{200}Hg ($r^2 = 0.56$, $p > 0.05$) toward the urban-industrial TGM values. Unlike the TGM concentration, the extent of anthropogenic influence appears to dictate the Δ^{199}Hg and Δ^{200}Hg. The absence of significant relationship between the TGM concentration and δ^{202}Hg ($r^2 = 0.04$, $p > 0.05$) can be explained by various atmospheric and biogeochemical processes resulting in MDF.[33]

The relationships between the TGM and few environmental factors (elevation, wind speed), and the TGM isotope ratios that are dependent on anthropogenic influence suggest that site-specific factors may partly govern the extent of anthropogenic Hg influence on our TGM. In addition to the TGM concentration, the TGM isotope ratios (δ^{202}Hg, Δ^{199}Hg) are weakly related to elevation (δ^{202}Hg; $r^2 = 0.14$, Δ^{199}Hg; $r^2 = 0.21$, both $p > 0.05$) and wind speed (δ^{202}Hg; $r^2 = 0.45$, Δ^{199}Hg; $r^2 = 0.51$, both $p > 0.05$), such that the mountain sites with high elevation and low wind speed have high TGM concentration and δ^{202}Hg and Δ^{199}Hg, similar to that of anthropogenic sources (Fig. S1†). The Δ^{199}Hg values alone correlated with the mean warmest temperature ($r^2 = 0.35$, $p > 0.05$) and humidity ($r^2 = 0.16$, $p > 0.05$), in that more negative Δ^{199}Hg (similar to background TGM) is observed at sites with high air temperature and low humidity (Fig. S1†).

Our results suggest that anthropogenically emitted TGM is effectively transported and trapped in high elevation mountains, where there is low wind speed. High wind speed often facilitates dispersion and depletion of locally and regionally transported TGM at high elevational mountains.[34–36] Kurz *et al.*[37] also reported night-time atmospheric inversion trapping of TGM in a remote mountain valley, leading to active Hg^0 uptake by vegetation. While all our measurements were taken during daytime, downward air mixing and subsequent TGM trapping in mountain valleys, where there is low wind speed, may increase TGM concentrations in the surrounding environment. The more negative Δ^{199}Hg observed at sites with high temperature and low humidity may be explained by Hg^0 re-emission

from foliage and/or forest floor (litter and soil), resembling the conditions of a remote mountain with little anthropogenic Hg influence. This finding aligns with Yuan *et al.*[11] as well as a number of other studies,[38–40] which identified a positive correlation between air–foliage Hg^0 exchange and temperature, as well as a negative correlation with humidity. This process would drive $\Delta^{199}Hg$ of Hg^0 to a slightly more negative value relative to Hg^{2+} *via* evaporation.[41] As such, while local anthropogenic influence mostly explains the site-specific TGM isotope ratios, certain environmental/climatic factors may enhance the extent of anthropogenic influence in high elevational mountain sites.

3.2. Forest media in relation to TGM

The foliage, litter, and topsoil THg concentrations range between 20 and 80 ng g^{-1} ($n = 22$), 44 and 125 ng g^{-1} ($n = 24$), and 108 and 320 ng g^{-1} ($n = 24$) (Table S4†), respectively, which are within the ranges of those reported in remote mountains of China and the U.S.[1,2,23] Similar to the TGM concentration, we do not observe distinct geographical difference or by proximity to local anthropogenic Hg emission sources in the forest THg concentrations. In relation to the TGM, a significant negative relationship is observed between the TGM and foliage THg concentration ($r^2 = 0.60$, $p < 0.05$) (Fig. S2†). This implies that high wind speeds not only reduce TGM concentrations in high elevation mountains by facilitating dispersion and depletion,[34–36] but also increase foliage THg concentrations by enhancing boundary layer conductance,[42] leading to higher transpiration and CO_2 assimilation rates.[43] The litter THg concentration does not correlate significantly with the foliage THg concentration ($r^2 = 0.04$, $p > 0.05$) but correlate positively with the topsoil THg ($r^2 = 0.51$, $p < 0.05$). While our TGM measurements do not cover the entire duration of plant growth cycle, the fact that TGM and THg concentrations in all forest media do not show distinct geographical pattern in relation to the proximity to local anthropogenic sources imply that local TGM concentration does not necessarily lead to high foliar Hg^0 uptake, resulting in elevated foliage and litter THg concentrations. The THg content in the litter, however, dictates the concentration of THg in the topsoil, possibly *via* litter decomposition and Hg sequestration into soil organic carbon.[44]

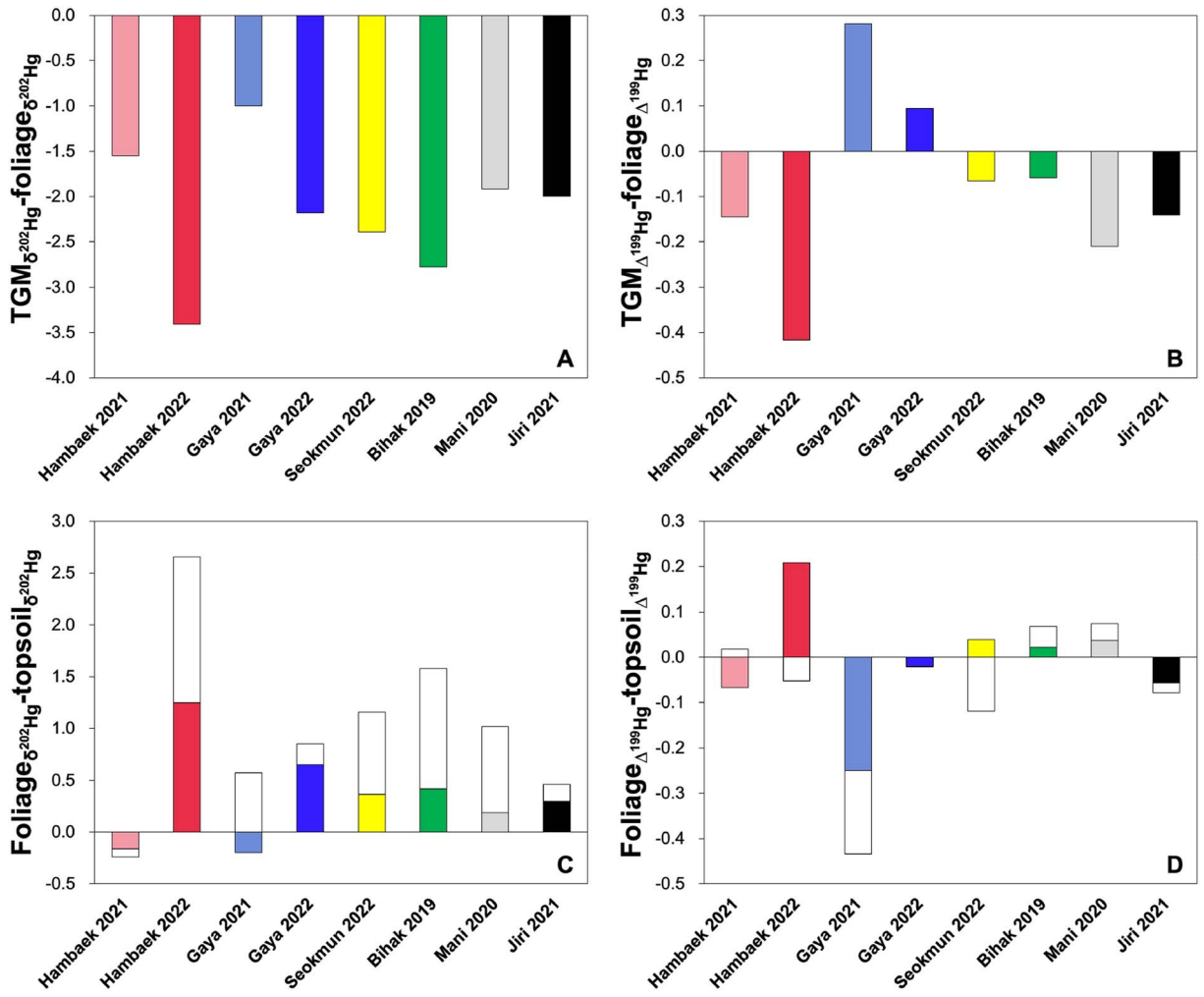

Fig. 3 The average magnitudes of $\delta^{202}Hg$ (A) and $\Delta^{199}Hg$ shift (B) from TGM to foliage at each mountain site of South Korea. The average magnitudes of $\delta^{202}Hg$ (C) and $\Delta^{199}Hg$ shift (D) from foliage to litter (colored bars) and to topsoil (white bars) at each mountain site.

In regard to Hg isotopes, all foliage, litter, and topsoil samples exhibit large negative δ^{202}Hg shifts and similar Δ^{199}Hg ranges relative to the TGM (Fig. 2C). To discuss the Hg isotope shifts between the TGM and foliage first, we find that the overall large negative δ^{202}Hg shift and small negative Δ^{199}Hg shift are consistent with MDF caused by Hg^0 uptake and oxidation by foliar tissues[10] and MIF mediated by Hg^{2+} photo-reduction and Hg^0 re-emission within foliage, respectively.[11,12] As illustrated in Fig. 3A, the site-specific δ^{202}Hg shifts between the TGM and foliage are consistently negative (−1.00 to −2.78‰). The Δ^{199}Hg shifts are small to negative (−0.06 and −0.42‰), except for Gaya (both 2021 and 2022), which display 0.10–0.28‰ higher Δ^{199}Hg in the foliage relative to their respective TGM (Fig. 3B). The positive Δ^{199}Hg shifts observed in Gaya are difficult to explain given that this site does not have noticeably high or low TGM concentration or THg in the forest media (Table S1 and S3†). We can only speculate that there may be less Hg^0 re-emission from foliage or some retention of Hg^{2+} on the foliage surface delivered *via* wet deposition and dry deposition, which typically have positive Δ^{199}Hg.[10,33] The overall pattern, however, indicates that the magnitude of δ^{202}Hg shift from TGM to foliage is negatively correlated with the TGM concentration ($r^2 = 0.41$, $p > 0.05$), but positively correlated with the foliage THg concentration ($r^2 = 0.46$, $p > 0.05$) (Fig. S3†). This is true even when considering the inter-annual differences in δ^{202}Hg shifts from TGM to foliage in Hambaek and Gaya and the associated TGM and foliage THg concentrations (Fig. 3A). The magnitude of Δ^{199}Hg shift is unrelated to the TGM and foliage THg (Fig. S3†). In line with the results of THg concentration, the site-specific TGM level does not govern the extent of foliar Hg^0 uptake. Instead, certain climatic/environmental factors may facilitate Hg^0 uptake, which subsequently cause large δ^{202}Hg shifts and elevated THg in the foliage.

Upon litterfall, Hg^{2+} retained within a litter is subjected to re-emission and/or sequestration by soil organic carbon *via* litter decomposition, both of which lead to opposite trends in δ^{202}Hg and Δ^{199}Hg. For instance, Yuan *et al.*[11] reported that Hg^0 re-emission during leaf senesces typically causes a lower δ^{202}Hg and a higher Δ^{199}Hg in the litter relative to fresh foliage. The documentation of a lower δ^{202}Hg and a lower Δ^{199}Hg in more matured leaves was attributed to re-mobilization of previously bound Hg within the leaf tissues, which is recycled following the reduction. Conversely, litter decomposition followed by microbial and dark abiotic Hg^{2+} reduction in soil results in a higher δ^{202}Hg and a slightly lower Δ^{199}Hg in Hg^{2+} retained within decomposing litter and soil.[13–15] In our study, negligible to significantly positive δ^{202}Hg shifts are observed in the litter and topsoil relative to the site-specific foliage δ^{202}Hg (foliage to litter; −0.20 to 1.25‰, litter to soil; −0.08 to 1.41‰) (Fig. 3C). The Δ^{199}Hg shifts are much more variable, with half of the sites (4 out of 8) displaying negative Δ^{199}Hg shifts and in similar magnitude to that of dark abiotic reduction (<−0.3‰) (Fig. 3D). The large negative Δ^{199}Hg shift from foliage, litter to topsoil in Gaya 2021 may be owing to the elevated Δ^{199}Hg in the foliage, as discussed in the previous section. The litter and topsoil in Bihak 2019, Mani 2020, and Hambaek 2022 exhibit, on average, positive Δ^{199}Hg shifts (0.07 to 0.16‰) from their respective foliage. Overall, the observed isotopic pattern across the forest media mimics active foliar Hg^0 uptake, litterfall, and subsequent decomposition, in which litter Hg provides the main source for soil Hg accumulation. Below, we evaluate in detail the site-specific environmental/climatic factors mediating foliar Hg^0 uptake, litter decomposition, and/or additional Hg deposition across the South Korean mountain sites.

3.3. Factors dictating foliar Hg^0 uptake

The relationships with five environmental/climatic factors suggest that wind speed is the strongest predictor of foliage Hg^0 uptake and its THg concentration (Fig. 4). When taking Hambaek 2022 out of the account, which shows anomalously large isotopic shifts from foliage, litter to topsoil (Fig. 2C), there is an improvement in the strength of correlation between wind speed

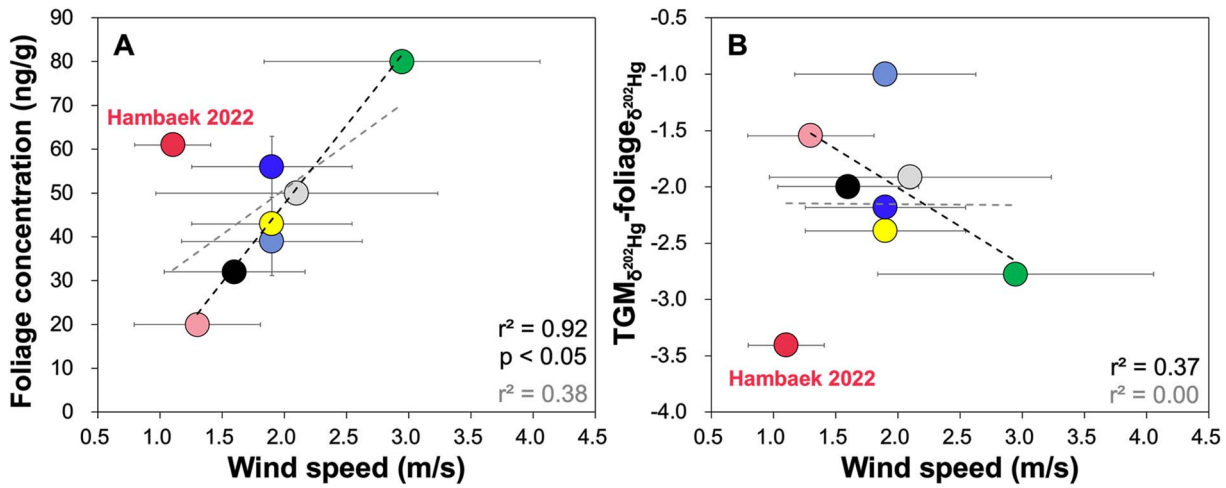

Fig. 4 Foliage THg concentration (A) and the magnitude of δ^{202}Hg shift from TGM to foliage (B) in relation to wind speed at each mountain site. The colors represent individual mountain site and are consistent with Fig. 3. The black dotted line represents the linear correlation without Hambaek 2022 and the grey dotted line represents the linear correlation across all mountain sites.

and the δ^{202}Hg shift associated with Hg^0 uptake by foliage (δ^{202}Hg of TGM minus δ^{202}Hg of foliage). The observed trend is opposite to that of site-specific TGM concentration. In the earlier section (Section 3.1), the mountain sites with high wind speed display low TGM concentration. These sites also appear to have elevated foliage THg concentration and the large associated δ^{202}Hg shift. This indicates that, while low wind speed explains the elevated TGM concentration, high wind speed facilitates foliage Hg^0 uptake possibly *via* physical mixing and Hg^0 passage through canopies. Our result somewhat contrasts a prior experimental study, which reported substantial Hg^0 releases from the leaf surface with increasing wind speed.[45] Few studies have also hypothesized that low wind speed would enhance foliar Hg^0 uptake, leading to enhanced forest Hg accumulation.[26,46] Our monitoring highlights the importance of wind speed as a predictor of site-specific foliage THg concentration and Hg isotope ratios, rather than the local TGM level. Across relatively narrow ranges of wind speed documented across the South Korean mountains, elevated local wind speed may be beneficial for enhancing Hg^0 passage through dense deciduous forest canopies. Wind speed as a factor dictating foliage THg and Hg isotope ratios, however, should be validated across a larger spatial scale and various terrestrial systems (*i.e.*, prairies, open fields).

Other environmental/climatic factors have only minor influences on the foliage THg concentration (Fig. S4†) and the associated δ^{202}Hg shift (Fig. S5†). This is likely owing to their intermittent (precipitation), counteracting (air temperature), and/or indirect (elevation, humidity) influences on Hg^0 uptake by foliage. For instance, high air temperature can increase the duration of stomata opening, thereby enhancing foliar Hg^0 uptake, as it is one of the heat tolerance mechanisms for reducing leaf temperature under periods of elevated air temperature.[47] High air temperature can, however, trigger stomata closure to mitigate water loss.[48] As for precipitation, prior evaluation of spatial Hg accumulation in the forest floor revealed a strong and dominant effect of precipitation, by increasing the overall biomass production, foliage available for Hg^0 uptake, and delivery to the forest floor.[1,2,21–24] As evident by the weak negative relationship between precipitation and our foliage THg concentration (Fig. S4†), high precipitation level may reduce Hg^0 uptake by scavenging Hg species from the atmosphere.[49,50] In this regard, precipitation, to a certain degree, may mediate bio-dilution effect by enhancing biomass production and the overall Hg^0 uptake but by decreasing a foliage-level Hg^0 accumulation. From the perspective of foliage, however, the effect of precipitation is minor relative to wind speed due to its intermittent role during the periods of rainfall.

3.4. Factors dictating Hg accumulation in the forest floor

The litter and topsoil THg concentrations and the magnitude of δ^{202}Hg shifts (all negligible to positive shifts) from foliage to topsoil are related to a wide range of environmental/climatic factors. Similar to the foliage, there are some improvements in the strength of correlations after excluding Hambaek 2022. We find that the mountain sites with high elevation, low wind speed, and low mean warmest temperature have elevated litter and topsoil THg concentrations (Fig. 5). High relative humidity has a negative effect on the litter THg but not on topsoil THg (Fig. S6†). The magnitudes of δ^{202}Hg shifts from foliage to topsoil, reflecting MDF mediated by biogeochemical processing of Hg^0 retained within a foliage, are smaller at sites with high elevation, low wind speed, and low mean warmest temperature. Precipitation has no effect on the litter and topsoil THg concentration and the sites with high annual precipitation display small magnitudes of δ^{202}Hg shifts from foliage to topsoil (Fig. S7†).

The relationships between various environmental/climatic factors and the litter and topsoil THg concentration and δ^{202}Hg shifts are somewhat consistent with the "cold trapping" effect reported in Mountain Leigong and Tibetan Plateau, China.[21,51] At each mountain site, the authors observed increasing soil THg with elevation and attributed this to enhanced Hg^{2+} input *via* fog water and precipitation, and suppressed Hg^0 re-emission from the forest floor, mediated by cold temperature. When evaluating across multiple mountain sites in South Korea, we observe a similar trend such that the mountains with high elevation, low wind speed, and low mean warmest temperature have characteristically elevated litter and topsoil THg concentrations. While the site-specific level of precipitation has no direct influence on litter and topsoil THg, the overall suppression of various biogeochemical processes leading to Hg^0 loss caused by cold temperature may be revealed by the small δ^{202}Hg shifts from foliage to topsoil.

From the perspective of biogeochemical processes facilitating Hg^0 loss from the forest floor, the observed trend highlights the importance of temperature and humidity. Zhang *et al.*,[25] using a passive exchange meter device, found that, under warm and humid conditions, a measurable proportion of Hg (~40%) fixed within a litter is re-emitted due to rapid turnover of labile organic matter mediated by decomposition. This process would lower litter THg level and reduce the amount of Hg available for soil sequestration. The low litter and topsoil THg concentration and large δ^{202}Hg shifts at sites with high temperature and wind speed resemble the effect of organic matter turnover leading to Hg^0 re-emission. Furthermore, the particularly strong negative correlation between wind speed and the topsoil THg ($r^2 = 0.60$, $p < 0.05$) and the positive correlation with the δ^{202}Hg shift ($r^2 = 0.77$, $p < 0.05$) indicate that Hg^0 evaporation,[41] which results in a positive δ^{202}Hg in the remaining Hg^{2+}, may play an additional role in lowering topsoil THg.

Similarly, the varying shifts in Δ^{199}Hg from foliage to topsoil can also be attributed to high wind speed and the high mean warmest temperature, leading to decomposition followed by re-emission of Hg^0. The only difference is whether the effect of decomposition is causing re-mobilization of previously bound Hg (negative shift in Δ^{199}Hg) or fast re-emission of recently deposited Hg^0 from the forest floor (positive shift in Δ^{199}Hg). Given that Bihak 2019, Mani 2020, and Hambaek 2022, which have some of the highest wind speeds and mean warmest temperatures, display positive Δ^{199}Hg shifts from foliage to

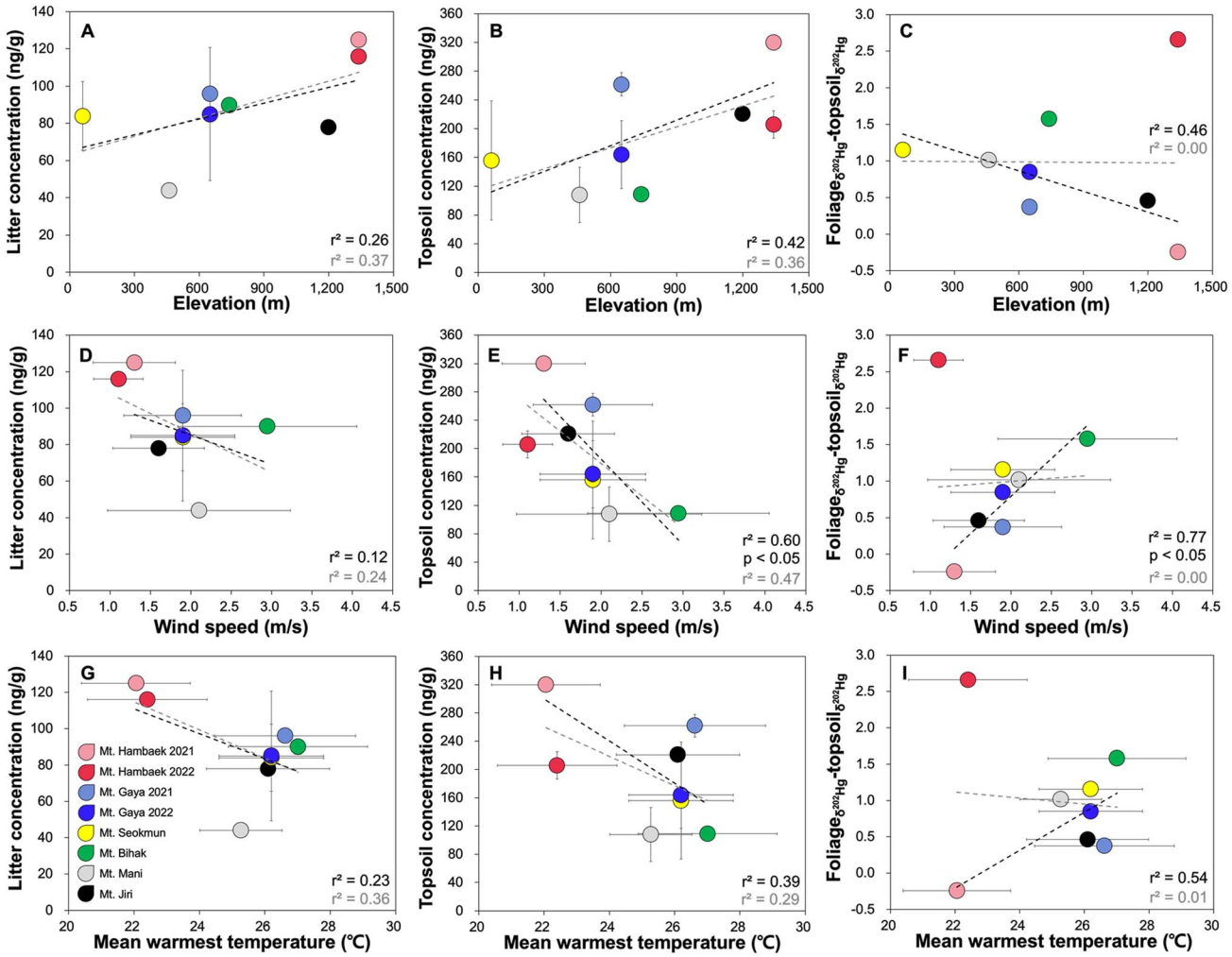

Fig. 5 Litter THg concentration in relation to elevation (A), wind speed (D), and the mean warmest temperature (G). Topsoil THg concentration in relation to elevation (B), wind speed (E), and the mean warmest temperature (H). The magnitude of δ^{202}Hg shift from foliage to topsoil in relation to elevation (C), wind speed (F), and the mean warmest temperature (I). The colors represent individual mountain site and are consistent with Fig. 3. The black dotted line represents the linear correlation without Hambaek 2022 and the grey dotted line represents the linear correlation across all mountain sites.

topsoil, we speculate that the effect of decomposition is offset by the fast Hg^0 re-emission from the forest floor. Alternatively, it is possible that wet and dry Hg^{2+} deposition explains the positive shifts observed from foliage to topsoil in Bihak 2019, Mani 2020, and Hambaek 2022. To evaluate this, we applied the average Δ^{200}Hg of our TGM (-0.037 ± 0.029) and the average Δ^{200}Hg of precipitation sampled from various regions of the world (0.16 ± 0.10)[10,52–62] as endmembers to the equations below quantify the contribution of Hg^0 and Hg^{2+} to the litter and topsoil in all mountain sites. Since significant Δ^{200}Hg anomalies occur exclusively *via* the atmospheric Hg^0 photo-oxidation,[17] Δ^{200}Hg has been used to distinguish between atmospheric Hg species affecting forest media.[16] The proportions of Hg^0 and Hg^{2+} are represented as $f_{Hg}{}^0$ and $f_{Hg}{}^{2+}$.

$$\Delta^{200}Hg_{sample} = \Delta^{200}Hg^{2+} \times f_{Hg^{2+}} + \Delta^{200}Hg^0 \times f_{Hg^0} \quad (5)$$

$$1 = f_{Hg^{2+}} + f_{Hg^0} \quad (6)$$

The results show that there are relatively small differences in % Hg^{2+} contribution to the litter (8–22%) and topsoil (16–31%) across the mountain sites (Table S5†). Bihak 2019, Mani 2020, and Hambaek 2022 also did not show distinctively higher % Hg^{2+} contribution (litter and topsoil combined; 28–38%) compared to other locations (26–41%). Consistent with the results of foliage, precipitation appears to have minor influences on foliar Hg^0 uptake, Hg^{2+} deposition as well as decomposition of Hg within the forest floor.

4. Conclusions & implications

The THg concentrations and Hg isotope ratios in TGM and forest media at six mountain sites of South Korea suggest that the extent of atmospheric Hg^0 uptake and accumulation within forests are dependent on mixtures of environmental/climatic factors rather than the local TGM concentration. We found that wind speed is the strongest predictor of foliage THg

concentration and the associated δ^{202}Hg shift, by enhancing Hg^0 passage through dense canopies. In the forest floor, decomposition, mediated by high temperature and humidity, and high wind speed facilitate Hg^0 re-emission, lower the forest floor THg, and enhance biogeochemically mediated MDF. In contrast to many prior studies, our study also demonstrates that precipitation has an intermittent and counteracting effect on forest Hg accumulation by lowering foliage-level THg and possibly by washing away Hg^{2+} deposited onto foliage/litter surfaces. The importance of wind speed acting as the primary factor for foliage THg and δ^{202}Hg shift should, however, be evaluated across various types of terrestrial systems including prairies and other open fields with high average wind speed.

The sensitivity of local environmental/climatic factors affecting the sources and the extent of forest Hg^0 uptake and accumulation merit the identification of key factors under climate change. Perhaps, the relative importance of these factors likely varies by region and/or biome type, and our study serves as a preliminary case for highlighting the importance of future environmental/climatic change modulating forest Hg uptake. It is suspected that South Korea will experience increased level and frequency of precipitation during summer months.[55] It is possible that precipitation leads to overall reduction in forest Hg by lowering foliage-level THg and by enhancing throughfall. Increased air and surface temperature *via* global warming may also expedite Hg^0 loss from the forest floor. As such, understanding factors that synergistically enhance or suppress atmospheric Hg^0 uptake and accumulation would aid better interpretation of the present and future forest Hg level and the spatiotemporal TGM concentrations over South Korea, dominated by forested mountains.

Conflicts of interest

There are no conflicts to declare.

Acknowledgements

This work was supported by the National Institute of Environmental Research R&D of the Korean Government (NIER-2022-01-01-074).

References

1 D. Obrist, D. W. Johnson, S. E. Lindberg, Y. Luo, O. Hararuk, R. Bracho, J. J. Battles, D. B. Dail, R. L. Edmonds, R. K. Monson, S. V. Ollinger, S. G. Pallardy, K. S. Pregitzer and D. E. Todd, Mercury distribution across 14 US forests. Part I: spatial patterns of 1concentrations in biomass, litter, and soils, *Environ. Sci. Technol.*, 2011, **45**, 3974–3981.

2 X. Wang, W. Yuan, C. J. Lin and X. Feng, Mercury cycling and isotopic fractionation in global forests, *Crit. Rev. Environ. Sci. Technol.*, 2022, **52**, 3763–3786.

3 J. Zhou, D. Obrist, A. Dastoor, M. Jiskra and A. Ryjkov, Mercury uptake by vegetation and impacts on global mercury cycling, *Nat. Rev. Earth Environ.*, 2021, **2**, 269–284.

4 A. W. Rea, S. E. Lindberg and G. J. Keeler, Dry deposition and foliar leaching of mercury and selected trace elements in deciduous forest throughfall, *Atmos. Environ.*, 2001, **35**, 3453–3462.

5 A. W. Rea, S. E. Lindberg, T. Scherbatskoy and G. J. Keeler, Mercury accumulation in foliage over time in two northern mixed-hardwood forests, *Water Air Soil Pollut.*, 2002, **133**, 49–67.

6 J. Stamenkovic and M. S. Gustin, Nonstomatal versus stomatal uptake of atmospheric mercury, *Environ. Sci. Technol.*, 2009, **43**, 1367–1372.

7 J. Zhou, S. W. Bollen, E. M. Roy, D. Y. Hollinger, T. Wang, J. T. Lee and D. Obrist, Comparing ecosystem gaseous elemental mercury fluxes over a deciduous and coniferous forest, *Nat. Commun.*, 2023, **14**, 2722.

8 N. E. Selin, Annu Rev Environ Resour, Global biogeochemical cycling of mercury: a review, *Annu Rev. Environ. Resour.*, 2009, **34**, 43–63.

9 D. Obrist, E. M. Roy, J. L. Harrison, C. F. Kwong, J. W. Munger, H. Moosmüller, C. D. Romero, S. Sun, J. Zhou and R. Commane, Previously unaccounted atmospheric mercury deposition in a midlatitude deciduous forest, *Proc. Natl. Acad. Sci. U. S. A.*, 2021, **118**, e2105477118.

10 J. D. Demers, J. D. Blum and D. R. Zak, Mercury isotopes in a forested ecosystem: implications for air-surface exchange dynamics and the global mercury cycle, *Glob. Biogeochem. Cycles*, 2013, **27**, 222–238.

11 W. Yuan, J. Sommar, C. J. Lin, X. Wang, K. Li, Y. Liu, H. Zhang, Z. Lu, C. Wu and X. Feng, Stable isotope evidence shows re-emission of elemental mercury vapor occurring after reductive loss from foliage, *Environ. Sci. Technol.*, 2019, **53**, 651–660.

12 B. Wang, W. Yuan, X. Wang, K. Li, C. J. Lin, P. Li, Z. Lu, X. Feng and J. Sommar, Canopy-level flux and vertical gradients of Hg0 stable isotopes in remote evergreen broadleaf forest show year-around net Hg^0 deposition, *Environ. Sci. Technol.*, 2022, **56**, 5950–5959.

13 S. Guédron, D. Amouroux, E. Tessier, C. Grimaldi, J. Barre, S. Berail, V. Perrot and M. Grimaldi, Mercury isotopic fractionation during pedogenesis in a tropical forest soil catena (French Guiana): Deciphering the impact of historical gold mining, *Environ. Sci. Technol.*, 2018, **52**, 11573–11582.

14 M. Jiskra, J. G. Wiederhold, U. Skyllberg, R. M. Kronberg, I. Hajdas and R. Kretzschmar, Mercury deposition and re-emission pathways in boreal forest soils investigated with Hg isotope signatures, *Environ. Sci. Technol.*, 2015, **49**, 7188–7196.

15 W. Yuan, X. Wang, C.-J. Lin, Q. Song, H. Zhang, F. Wu, N. Liu, H. Lu and X. Feng, Deposition and Re-Emission of Atmospheric Elemental Mercury over the Tropical Forest Floor, *Environ. Sci. Technol.*, 2023, **29**, 10686–10695.

16 B. A. Bergquist and J. D. Blum, Mass-dependent and-independent fractionation of Hg isotopes by photoreduction in aquatic systems, *Science*, 2007, **318**, 417–420.

17 H. Cai and J. Chen, Mass-independent fractionation of even mercury isotopes, *Sci. Bull.*, 2016, **61**, 116–124.
18 G. E. Woerndle, M. Tsz-Ki Tsui, S. D. Sebestyen, J. D. Blum, X. Nie and R. K. Kolka, New insights on ecosystem mercury cycling revealed by stable isotopes of mercury in water flowing from a headwater peatland catchment, *Environ. Sci. Technol.*, 2018, **52**, 1854–1861.
19 W. Zheng and H. Hintelmann, Nuclear field shift effect in isotope fractionation of mercury during abiotic reduction in the absence of light, *J. Phys. Chem. A*, 2010, **114**, 4238–4245.
20 W. Zheng, J. D. Demers, X. Lu, B. A. Bergquist, A. D. Anbar, J. D. Blum and B. Gu, Mercury stable isotope fractionation during abiotic dark oxidation in the presence of thiols and natural organic matter, *Environ. Sci. Technol.*, 2018, **53**, 1853–1862.
21 X. Wang, J. Luo, R. Yin, W. Yuan, C. J. Lin, J. Sommar, X. Feng, H. Wang and C. Lin, Using mercury isotopes to understand mercury accumulation in the montane forest floor of the Eastern Tibetan Plateau, *Environ. Sci. Technol.*, 2017, **51**, 801–809.
22 X. Wang, W. Yuan, Z. Lu, C. J. Lin, R. Yin, F. Li and X. Feng, Effects of precipitation on mercury accumulation on subtropical montane forest floor: implications on climate forcing, *J. Geophys. Res. Biogeosci.*, 2019, **124**, 959–972.
23 X. Zehua, Z. Wang and X. Zhang, Mapping the forest litterfall mercury deposition in China, *Sci. Total Environ.*, 2022, **839**, 156288.
24 W. Zheng, D. Obrist, D. Weis and B. A. Bergquist, Mercury isotope compositions across North American forests, *Global Biogeochem. Cycles*, 2016, **30**, 1475–1492.
25 H. Zhang, L. Nizzetto, X. Feng, K. Borgå, J. Sommar, X. Fu, H. Zhang, G. Zhang and T. Larssen, Assessing air–surface exchange and fate of mercury in a subtropical forest using a novel passive exchange-meter device, *Environ. Sci. Technol.*, 2019, **53**, 4869–4879.
26 X. Fu, H. Zhang, C. Liu, H. Zhang, C. J. Lin and X. Feng, Significant seasonal variations in isotopic composition of atmospheric total gaseous mercury at forest sites in China caused by vegetation and mercury sources, *Environ. Sci. Technol.*, 2019, **53**, 13748–13756.
27 Korea Forest Service, *Forest Basic Statistics 2020*, Seoul, Korea, 2021.
28 H. Lee, S. Y. Kwon, J. Kam, K. Lee, X. Fu, I. G. Cho and S. D. Choi, Isotopic investigation of sources and processes affecting gaseous and particulate bound mercury in the east coast, South Korea, *Sci. Total Environ.*, 2023, **891**, 164404.
29 J.-H. Sung, J.-S. Oh, S.-K. Back, B.-M. Jeong, H.-N. Jang, Y.-C. Seo and S.-H. Kim, Estimation of mercury emission from major sources in annex D of Minamata convention and future trend, *J. Korean Soc. Atmos.*, 2016, **32**, 193–207.
30 U. S. EPA, *Method 1631, Revision E: Mercury in Water by Oxidation, Purge and Trap, and Cold Vapor Atomic Fluorescence Spectrometry, EPA-821-R-02-019*, U.S. Environmental Protection Agency, Office of Water, Washington, D.C., 2002.
31 J. D. Blum and M. W. Johnson, Recent Developments in Mercury Stable Isotope Analysis, *Rev. Mineral. Geochem.*, 2017, **82**, 733–757.
32 J. D. Blum and B. A. Bergquist, Reporting of variations in the natural isotopic composition of mercury, *Anal. Bioanal.*, 2007, **388**, 353–359.
33 S. Y. Kwon, J. D. Blum, R. Yin, M. T. K. Tsui, Y. H. Yang and J. W. Choi, Mercury stable isotopes for monitoring the effectiveness of the Minamata Convention on Mercury, *Earth Sci. Rev.*, 2020, **203**, 103111.
34 X. W. Fu, X. Feng, Z. Q. Dong, R. S. Yin, J. X. Wang, Z. R. Yang and H. Zhang, Atmospheric gaseous elemental mercury (GEM) concentrations and mercury depositions at a high-altitude mountain peak in south China, *Atmos. Chem. Phys.*, 2010, **10**, 2425–2437.
35 X. Fu, W. Zhu, H. Zhang, J. Sommar, B. Yu, X. Yang, X. Wang, C.-J. Lin and X. Feng, Depletion of atmospheric gaseous elemental mercury by plant uptake at Mt. Changbai, Northeast China, *Atmos. Chem. Phys.*, 2016, **16**, 12861–12873.
36 J. Zhu, T. Wang, R. Talbot, H. Mao, C. B. Hall, X. Yang, C. Fu, B. Zhuang, S. Li, Y. Han and X. Huang, Characteristics of atmospheric total gaseous mercury (TGM) observed in urban Nanjing, China, *Atmos. Chem. Phys.*, 2012, **12**, 12103–12118.
37 A. Y. Kurz, J. D. Blum, L. E. Gratz and D. A. Jaffe, Contrasting controls on the diel isotopic variation of Hg^0 at two high elevation sites in the Western United States, *Environ. Sci. Technol.*, 2020, **54**, 10502–10513.
38 M. D. Almeida, R. V. Marins, H. H. M. Paraquetti, W. R. Bastos and L. D. Lacerda, Mercury degassing from forested and open field soils in Rondônia, Western Amazon, Brazil, *Chemosphere*, 2009, **77**, 60–66.
39 T. Kuiken, M. Gustin, H. Zhang, S. Lindberg and B. Sedinger, Mercury emission from terrestrial background surfaces in the eastern USA. II: Air/surface exchange of mercury within forests from South Carolina to New England, *Appl. Geochem.*, 2008, **23**, 356–368.
40 M. Mazur, C. P. J. Mitchell, C. S. Eckley, S. L. Eggert, R. K. Kolka, S. D. Sebestyen and E. B. Swain, Gaseous mercury fluxes from forest soils in response to forest harvesting intensity: a field manipulation experiment, *Sci. Total Environ.*, 2014, **496**, 678–687.
41 N. Estrade, J. Carignan, J. E. Sonke and O. F. X. Donard, Mercury isotope fractionation during liquid–vapor evaporation experiments, *Geochim. Cosmochim. Acta*, 2009, **73**, 2693–2711.
42 T. A. Martin, T. M. Hinckley, F. C. Meinzer and D. G. Sprugel, Boundary layer conductance, leaf temperature and transpiration of Abies amabilis branches, *Tree Physiol.*, 1999, **19**, 435–443.
43 S. J. Schymanski and D. Or, Wind increases leaf water use efficiency, *Plant Cell Environ.*, 2016, **39**, 1448–1459.
44 D. F. Grigal, Mercury sequestration in forests and peatlands: a review, *J. Environ. Qual.*, 2003, **32**, 393–405.
45 A. Gillis and D. R. Miller, Some potential errors in the measurement of mercury gas exchange at the soil surface

using a dynamic flux chamber, *Sci. Total Environ.*, 2000, **260**(1–3), 181–189.

46 X. Fu, N. Marusczak, X. Wang, F. Gheusi and J. E. Sonke, Isotopic composition of gaseous elemental mercury in the free troposphere of the Pic du Midi Observatory, *Environ. Sci. Technol.*, 2016, **50**, 5641–5650.

47 K. I. Kostaki, A. Coupel-Ledru, V. C. Bonnell, M. Gustavsson, P. Sun, F. J. McLaughlin, D. P. Fraser, D. H. McLachlan, A. M. Hetherington, A. N. Dodd and K. A. Franklin, Guard cells integrate light and temperature signals to control stomatal aperture, *Plant Physiol.*, 2020, **182**, 1404–1419.

48 A. D. Friend, Use of a model of photosynthesis and leaf microenvironment to predict optimal stomatal conductance and leaf nitrogen partitioning, *Plant Cell Environ.*, 1991, **14**, 895–905.

49 M. Sakata and K. Asakura, Estimating contribution of precipitation scavenging of atmospheric particulate mercury to mercury wet deposition in Japan, *Atmos. Environ.*, 2007, **41**, 1669–1680.

50 Y. S. Seo, Y. J. Han, H. D. Choi, T. M. Holsen and S. M. Yi, Characteristics of total mercury (TM) wet deposition: scavenging of atmospheric mercury species, *Atmos. Environ.*, 2012, **49**, 69–76.

51 H. Zhang, R. S. Yin, X. Bin Feng, J. Sommar, C. W. N. Anderson, A. Sapkota, X. W. Fu and T. Larssen, Atmospheric mercury inputs in montane soils increase with elevation: evidence from mercury isotope signatures, *Sci. Rep.*, 2013, **3**, 3322.

52 S. Yuan, Y. Zhang, J. Chen, S. Kang, J. Zhang, X. Feng, H. Cai, Z. Wang, Z. Wang and Q. Huang, Large variation of mercury isotope composition during a single precipitation event at Lhasa City, Tibetan Plateau, China, *Proced. Earth Plan. Sci.*, 2015, **13**, 282–286.

53 J. Chen, H. Hintelmann, X. Feng and B. Dimock, Unusual fractionation of both odd and even mercury isotopes in precipitation from Peterborough, ON, Canada, *Geochim. Cosmochim. Acta*, 2012, **90**, 33–46.

54 P. M. Donovan, J. D. Blum, D. Yee, G. E. Gehrke and M. B. Singer, An isotopic record of mercury in San Francisco Bay sediment, *Chem. Geol.*, 2013, **349**, 87–98.

55 L. S. Sherman, J. D. Blum, G. J. Keeler, J. D. Demers and J. T. Dvonch, Investigation of local mercury deposition from a coal-fired power plant using mercury isotopes, *Environ. Sci. Technol.*, 2012, **46**, 382–390.

56 L. S. Sherman, J. D. Blum, J. T. Dvonch, L. E. Gratz and M. S. Landis, The use of Pb, Sr, and Hg isotopes in Great Lakes precipitation as a tool for pollution source attribution, *Sci. Total Environ.*, 2015, **502**, 362–374.

57 L. E. Gratz, G. J. Keeler, J. D. Blum and L. S. Sherman, Isotopic composition and fractionation of mercury in Great Lakes precipitation and ambient air, *Environ. Sci. Technol.*, 2010, **20**, 7764–7770.

58 Z. Wang, J. Chen, X. Feng, H. Hintelmann, S. Yuan, H. Cai, Q. Huang, S. Wang and F. Wang, Mass-dependent and mass-independent fractionation of mercury isotopes in precipitation from Guiyang, SW China, *C. R. Geosci.*, 2015, **347**, 358–367.

59 S. Huang, L. Sun, T. Zhou, D. Yuan, B. Du and X. Sun, Natural stable isotopic compositions of mercury in aerosols and wet precipitations around a coal-fired power plant in Xiamen, southeast China, *Atmos. Environ.*, 2018, **173**, 72–80.

60 L. C. Motta, J. D. Blum, M. W. Johnson, B. P. Umhau, B. N. Popp, S. J. Washburn, J. C. Drazen, C. R. Benitez-Nelson, C. C. S. Hannides, H. G. Close and C. H. Lamborg, Mercury cycling in the North Pacific Subtropical Gyre as revealed by mercury stable isotope ratios, *Global Biogeochem.*, 2019, **33**, 777–794.

61 M. Enrico, G. L. Roux, N. Marusczak, L. E. Heimbürger, A. Claustres, X. Fu, R. Sun and J. E. Sonke, Atmospheric mercury transfer to peat bogs dominated by gaseous elemental mercury dry deposition, *Environ. Sci. Technol.*, 2016, **50**, 2405–2412.

62 X. Fu, M. Jiskra, X. Yang, N. Marusczak, M. Enrico, J. Chmeleff, L.-E. Heimbürger-Boavida, F. Gheusi and J. E. Sonke, Mass-independent fractionation of even and odd mercury isotopes during atmospheric mercury redox reactions, *Environ. Sci. Technol.*, 2021, **55**, 10164–10174.